Title

Accounting for radiative forcing from albedo change in future global land-use scenarios

Journal

Climatic Change, 131(4)

ISSN

0165-0009

Authors

Jones, Andrew D
Calvin, Katherine V
Collins, William D
et al.

Publication Date

2015-08-01

DOI

10.1007/s10584-015-1411-5

Peer reviewed

Accounting for radiative forcing from albedo change in future global land-use scenarios

- Authors
- Authors and affiliations

- Andrew D. Jones
- Katherine V. Calvin
- William D. Collins
- James Edmonds

Abstract

We demonstrate the effectiveness of a new method for quantifying radiative forcing from land use and land cover change (LULCC) within an integrated assessment model, the Global Change Assessment Model (GCAM). The method relies on geographically differentiated estimates of radiative forcing from albedo change associated with major land cover transitions derived from the Community Earth System Model. We find that conversion of 1 km^2 of woody vegetation (forest and shrublands) to non-woody vegetation (crops and grassland) yields between 0 and -0.71 nW/m^2 of globally averaged radiative forcing determined by the vegetation characteristics, snow dynamics, and atmospheric radiation environment characteristic within each of 151 regions we consider globally. Across a set of scenarios designed to span a range of potential future LULCC, we find LULCC forcing ranging from -0.06 to -0.29 W/m^2 by 2070 depending on assumptions regarding future crop yield growth and whether climate policy favors afforestation or bioenergy crops. Inclusion of this previously uncounted forcing in the policy targets driving future climate mitigation efforts leads to changes in fossil fuel emissions on the order of 1.5 PgC/yr by 2070 for a climate forcing limit of 4.5 Wm^{-2}, corresponding to a 12–67 % change in fossil fuel emissions depending on the scenario. Scenarios with significant afforestation must compensate for albedo-induced warming through additional emissions reductions, and scenarios with significant deforestation need not mitigate as aggressively due to albedo-induced cooling. In all scenarios considered, inclusion of albedo forcing in policy targets increases forest and shrub cover globally.

Keywords

Land Cover Change Woody Vegetation Carbon Price Earth System Model Bioenergy Crop

These keywords were added by machine and not by the authors. This process is experimental and the keywords may be updated as the learning algorithm improves.

Andrew D. Jones and Katherine V. Calvin contributed equally to this work.

1 Introduction

In addition to their effects on atmospheric carbon dioxide, land-use and land cover changes (LULCCs) are known to influence climate directly by altering surface physical properties such as the amount of reflected sunlight (albedo) or the amount of water transpired from soils to the atmosphere (Foley et al. 2005; Bonan 2008). These effects are most pronounced at regional scales (Feddema et al. 2005; Foley et al. 2005; Bonan 2008; Hallgren et al. 2013; Brovkin et al. 2013), but some scenarios of future LULCC have been shown to affect global mean quantities such as temperature and precipitation (Jones et al. 2013a; Davies-Barnard et al. 2014).

Many studies have discussed the relative climate benefits of various LULCCs based on the balance of direct physical and carbon cycle effects (Bala et al. 2007; Pongratz et al. 2010; Arora and Montenegro 2011). For instance, tropical deforestation is thought to have a net warming effect due to the combination of carbon dioxide emissions and decreased evapotranspiration, while Boreal deforestation is thought to have a net neutral or net cooling effect due to a strong albedo signal that counteracts the carbon cycle effects. However, past Boreal deforestation may have favored areas with less snow cover and therefore relatively weaker albedo effects (Pongratz et al. 2011). By similar logic, the lifecycle climate effect of various biofuels depends on both the carbon cycle and direct physical effects of land conversion (Caiazzo et al. 2014).

Policies that account for, encourage, or discourage particular LULCC activities based on their non-CO_2 climate effects might shift the balance between afforestation and bioenergy crop cultivation or might alter the controls on fossil fuel emissions to meet their more comprehensive forcing targets. For example, consideration of the positive albedo forcing associated with conversion of grassland to forest at high latitudes would require deeper emissions cuts to achieve the same radiative forcing target. Exploring the dynamics of such hypothetical policies could inform decision-making and shed light on the relative importance of non-CO_2 LULCC effects compared to other climate drivers.

Integrated assessment models (IAMs) are designed to project the co-evolution of human energy, agricultural, and land-use systems and their consequent climate forcings subject to various policy constraints. Thus, IAMs could be ideal tools for exploring a rich set of LULCC policies that consider multiple forcing mechanisms. However, IAMs do not presently account for

the non-CO_2 effects of LULCC on climate. This exclusion complicates both the reliable quantification of climate outcomes from alternative LULCC scenarios as well as the development of comprehensive and nuanced policy specifications based on these scenarios.

For example, Jones et al. (2013a) showed in the context of the Representative Concentration Pathways (RCPs; (van Vuuren et al. 2011) utilized in the Fifth Coupled Model Intercomparison Project (CMIP5; (Taylor et al. 2012) that it is possible to reach the same nominal radiative forcing level in 2100 with substantially different patterns of LULCC, and consequently very different patterns of global and regional climate. The forcing levels reported by IAMs and used to drive internal climate policies for the RCPs did not include direct physical forcing from LULCC.[1] Thus, a mechanism to calculate forcing from LULCC within IAMs would enable differentiating among such scenarios without the need for additional climate and Earth system model (ESM) simulations. It would also help to identify just how different LULCC must be among scenarios to make a difference for global forcing and therefore climate.

However, accounting for the full non-CO_2 climate effects of LULCC in IAMs – particularly using metrics such as global mean radiative forcing – is challenging for several reasons. Some of the climate effects of LULCC (e.g., changes in evapotranspiration) are not directly linked to a change in the Earth's radiative budget and therefore cannot be quantified in terms of radiative forcing (Pielke et al. 2002). For those effects that can be quantified in terms of radiative forcing, the regional nature of LULCC forcing relative to that of well-mixed greenhouse gases like CO_2means that a unit of LULCC forcing can imply a very different pattern of climate change depending on where the LULCC occurs. Given this regionality, it is possible to construct net neutral forcing scenarios combining negative forcing from LULCC and positive forcing from greenhouse gases yet still induce globally significant patterns of climate change (Jones et al. 2013b). Thus caution should be taken when interpreting the sum of forcings from diverse climate perturbations.

Despite these challenges, radiative forcing remains the dominant paradigm for characterizing the overall scale of climate perturbations associated with human activities or other external climate influences. Its strength lies in its simplicity and the fact that it can often be calculated without the need for climate models and therefore avoids model-specific uncertainties. We note that IAMs currently include forcing estimates from aerosols such as sulfur dioxide, black carbon, and mineral dust that are also regional in nature and have been shown to exhibit forcing-response relationships that vary under different conditions, e.g., the altitude of black carbon aerosols (Ban-Weiss et al. (2011). It follows that policies based on global mean radiative forcing could yield unexpected climate outcomes, particularly at regional scales. A

systematic examination of such policies within IAMs, their implied climate outcomes based on global mean radiative forcing, and their regional climate effects simulated using climate and Earth system models would help assess the utility of global mean radiative forcing as a comprehensive climate change metric. However, as noted above, examining such policies within IAMs first requires an accounting of the relevant forcings.

Here we present a method for calculating global mean radiative forcing from regional LULCC within an IAM, the Global Change Assessment Model (GCAM) (Calvin et al. 2011). We use these calculations to characterize the scale of non-CO_2 climate effects for various scenarios of future LULCC and to explore the implications of including these effects in hypothetical climate-change mitigation policies.

2 Methods

2.1 Forcing factors

Our approach is to develop geographically specific radiative forcing factors for use in GCAM. We focus in this initial version on the large albedo signal associated with conversion of woody vegetation (forests and/or shrublands) to non-woody vegetation (grassland and/or cropland). We employ GCAM 3.0 (Wise et al. 2014) which represents land-use dynamics within 151 sub-regions formed by intersecting 18 global agro-ecological zones (AEZs) with 14 geopolitical regions. The AEZs are regions of relatively uniform bio-climatic characteristics derived from a combination of growing season length and temperature data (Lee et al. 2005; Monfreda et al. 2009).

Within each of these 151 regions, we obtain estimates of radiative forcing due to land conversion from woody vegetation to non-woody vegetation. We do this through a series of simulations with the Community Earth System Model (CESM) (Hurrell et al. 2013) a global earth system model. The simulations are designed to isolate the surface albedo and corresponding top-of-atmosphere radiative flux change associated with changing the mix of woody vegetation and non-woody vegetation present within each approximately 1-degree gridcell, using methods similar to those described in Jones et al. (2013a).

We begin by generating a self-consistent atmospheric control data set for the present day climate by running CESM for 11 model years with specified sea surface temperatures corresponding to the period 1995–2005 (Hurrell et al. 2008). Land cover, aerosol concentrations, and greenhouse gas concentrations are held at year 2000 levels. From this simulation, we save detailed data (e.g., precipitation, surface insolation) for driving the Community Land Model (CLM) (Lawrence et al. 2011), the land surface

component of CESM, in an offline mode. We also save the three dimensional atmospheric state variables necessary to drive an offline version (Conley et al. 2013) of the Community Atmosphere Model's (CAM's) (Park et al. 2014) radiative transfer scheme (Iacono et al. 2008). For computational and data management reasons, we save the three-dimensional atmospheric state every 73 timesteps, which corresponds to 1.5 days plus 30 min. This scheme results in a sampling structure that is evenly distributed throughout the seasonal and diurnal cycles.

Next, we consider two offline land model simulation in which the vegetated portion of each grid cell has been filled entirely with either woody vegetation or non-woody vegetation, preserving the gridcell-specific relative ratios of plant functional types within the categories of woody and non-woody vegetation. The seasonal cycle of leaf and stem area by plant functional type and gridcell is specified based on MODIS satellite data (Lawrence and Chase 2007). The surface albedos from these simulations are then used to drive two offline radiative transfer simulations in which all other atmospheric conditions are held constant based on the atmospheric control simulation.

The time-averaged difference in top-of-atmosphere net radiation between these radiative transfer simulations over any particular gridcell yields the instantaneous forcing associated with conversion of all vegetated area in the gridcell from woody to non-woody vegetation. We discard the first simulation year to account for atmospheric spinup and we also discard the 6th year due to partially missing data for that year. Within each GCAM region, we take the total change in top-of-atmosphere radiation, normalize by the ratio of region area to global area (including all land and oceans), and divide by the total vegetated area converted to obtain the global mean forcing per unit of land conversion for that region.

Within GCAM, future changes in albedo forcing are calculated by applying these factors to GCAM's land cover change at each time step in each region. We note that this version of GCAM represents several crop types, yet has a single landcover class for each of forests, shrubs, and pasture. We take woody vegetation to be the sum of forest and shrub area within GCAM and non-woody vegetation to be the sum of pasture and crop land. The global sum of these forcing changes is passed to the simplified climate module within GCAM, the MAGICC model (Meinshausen et al. 2011), where they modify the historical albedo forcing value of -0.2 W/m^2.

2.2 Scenarios

The scenarios developed all use the GCAM model, which operates in a transient mode, solving every 5 years from 2005 to 2070. Each of the scenarios developed for this paper use the same set of basic input

assumptions (e.g., population, labor productivity growth, resource availability, technology availability, technology cost, agricultural productivity, etc.) in GCAM. Each of these input assumptions evolves over time, such that the world simulated in 2070 is substantially different from the world simulated in 2005. For example, global population in 2070 is 9.2 billion, compared to 6.5 billion in 2005. For each five-year period, GCAM computes energy supply, energy demand, agriculture supply, agriculture demand, land use, land cover, emissions, and globally averaged climate. These quantities are calculated by adjusting prices until all supplies and demands are equilibrated. In this particular exercise, we are assuming the coupling with climate is one way. That is, energy, agriculture and land affect the climate system through changes in emissions and in some scenarios changes in land cover (see below), but climate does not affect the energy, agriculture, or land systems in this set of scenarios.

We consider three ways of handling albedo in GCAM: default, diagnostic, and interactive. In the default mode, albedo is held constant at the historical value of -0.2 W/m^2 even in scenarios with dramatic future changes in land cover. This is the version of the model that predates the modifications described above. In diagnostic mode (-DIAG), future albedo forcing changes are calculated internally but are omitted from policy targets and therefore do not alter the dynamics of energy and land use over the course of the simulation. In interactive mode (-INT), the calculated future albedo forcings are included in policy targets and therefore influence the mix of mitigation strategies introduced to meet those targets. We note that while the models used to generate the RCPs discarded historic albedo forcing altogether in their policy target calculations, we include fixed historic forcing in policy targets in all modes. We do this for consistency with the interactive scenarios. Using this approach, the difference between the interactive and diagnostic scenarios reflects the added effect of future albedo change.

We examine three scenarios types: 1) a reference case with no climate policy, which is an update of the reference scenario in Thomson, et al. (2011); 2) a climate stabilization scenario that limits climate forcing to 4.5 W/m^2 via a universal carbon tax (UCT) that taxes emissions of both fossil fuel and terrestrial carbon emissions at the same rate; and 3) another 4.5 W/m^2stabilization scenario employing a carbon tax on fossil fuel and industrial emissions only (FFICT). The UCT scenario is comparable to the standard RCP4.5 in its formulation but differs in its implementation since we adopt the new GCAM version 3.0 in place of older version used to generate the official RCP4.5. We examine each of these policy scenarios in both the diagnostic and interactive modes of introducing albedo forcing into GCAM. This yields five core scenarios comprised of the reference case (REF)_and the four combinations of stabilization scenarios and forcing modes denoted by UCT-DIAG, UCT-INT, FFICT-DIAG, and FFICT-INT. As a sensitivity analysis, we consider variants of FFICT-DIAG, and FFICT-INT denoted by FFICT-LOW-

DIAG and FFICT-LOW-INT in which agricultural yields do not increase over the 21st century as in the other scenarios. We expect this pair of additional scenarios to yield the highest rate of deforestation since additional land will be required to meet food and biofuel demands.

We note that while we include albedo forcing in the policy targets in interactive mode, the tax mechanism is directed at greenhouse gas emissions. This means that land-use change decisions are not directly taxed or credited for their albedo forcing implications, but rather influence mitigation strategies indirectly by effectively tightening or loosening the forcing target. Directly influencing land-use decisions would require either conversion of albedo forcing to carbon-dioxide equivalents, or the replacement of the carbon tax with a radiative forcing tax – both interesting and relevant options that could be explored in future work.

3 Results

The forcing factors (presented in Fig. 1) vary significantly by region. The magnitudes of these forcings are greatest in the Boreal forest regions and the Tibetan plateau where the contrast between dark trees and light snow is most pronounced. At very high latitudes, where woody vegetation is less dense and incident solar radiation is relatively low, forcing diminishes. We note that these factors are expressed in terms of global forcing per unit of converted area and that the amount of woody vegetation available to be converted may be quite low in some regions, e.g., deserts.

Open image in new window

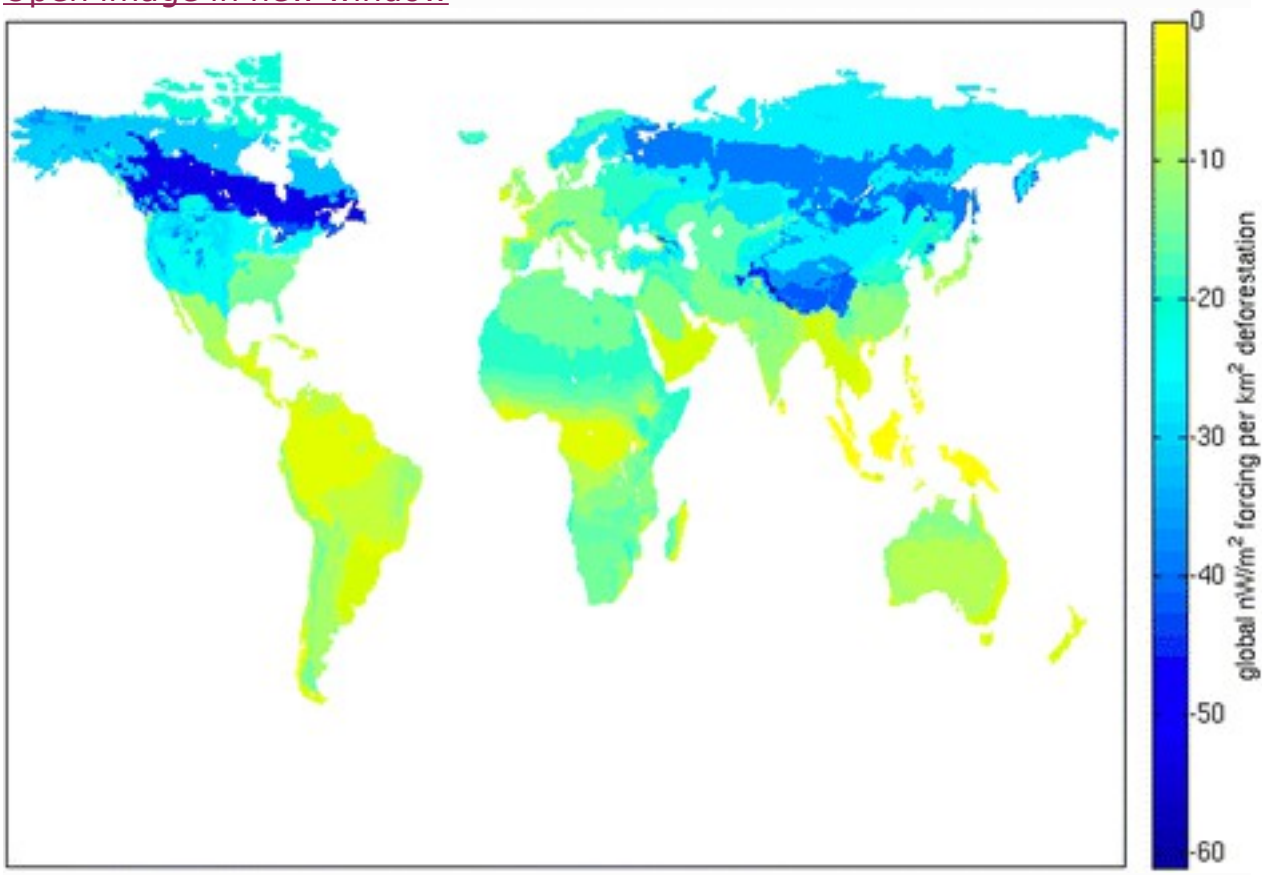

Fig. 1
Model-derived estimates of radiative forcing due to land conversion from woody vegetation (forest or shrub) to non-woody vegetation (grass or crop). Mean values are shown for each of the agroecological zones used to represent land-use within the Global Change Assessment Model. Values signify the global change in forcing (in nW/m^2) for each km^2 of land conversion in a given location

As in previous studies (Wise et al. 2009; Calvin et al. 2014), we find that the UCT scenarios feature afforestation as a carbon mitigation strategy (see Fig. 2) with correspondingly lower bioenergy crop utilization compared to a reference scenario with no policy. The FFICT scenarios, on the other hand, feature deforestation and expanded use of bioenergy crops. In contrast to previous studies, though, we are now able to estimate the albedo forcing change associated with these land cover changes (Fig. 3). Additional forest cover in the UCT-DIAG scenario induces a positive radiative forcing of 0.13 W/m^2 by 2070,[2] reducing the negative forcing from historical LULCC from −0.2 to −0.07 W/m^2. Deforestation in the FFICT-DIAG and FFICT-LOW-DIAG scenarios reduces radiative forcing by −0.05 W/m^2 and −0.09 W/m^2, respectively, for a net albedo forcing including historical LULCC of −0.25 W/m^2 and −0.29 W/m^2, respectively.

Open image in new window

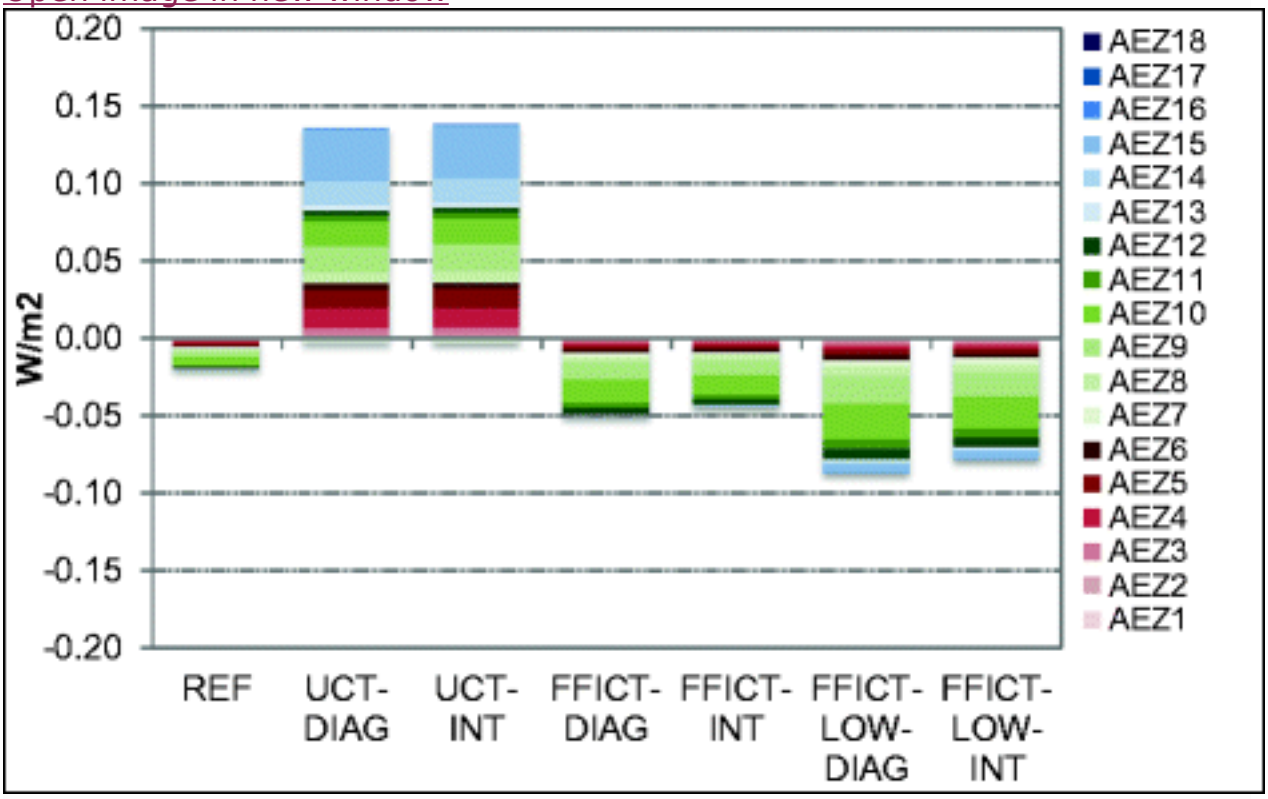

Fig. 2

Change in woody vegetation cover (forest and shrub) in 2070 relative to 2005 by agro-ecological zone (AEZ) for each scenario. AEZs 1–6 are tropical, AEZs 7–12 are temperate, and AEZs 13–18 are Boreal

Open image in new window

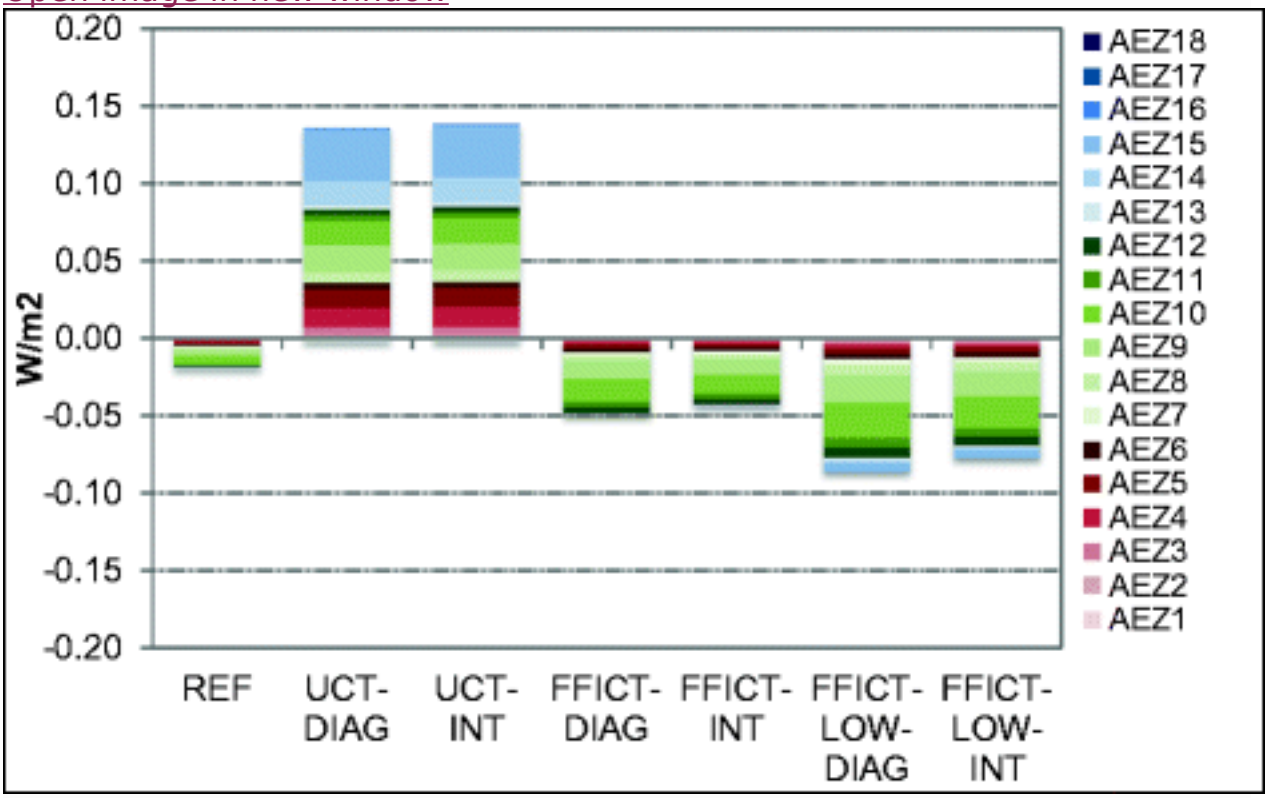

Fig. 3
Change in global radiative forcing from albedo change in 2070 relative to 2005 by agro-ecological zone (AEZ) for each scenario. AEZs 1–6 are tropical, AEZs 7–12 are temperate, and AEZs 13–18 are Boreal

Interactive versions of each scenario yield slightly higher (more positive) forcing levels and slightly higher overall forest and shrub cover than their diagnostic scenario counterparts. The dynamics underlying this feedback can be seen by examining the carbon price changes and shifting mitigation strategies employed in each scenario. In the UCT-INT scenario, additional forcing from afforestation makes the 4.5 W/m^2 target more difficult to meet, thereby increasing the carbon price (Fig. 4) and forcing the energy and industrial sectors to mitigate more aggressively (Fig. 5). Fossil fuel and industrial carbon emissions are reduced by 1.3 PgC/yr (12 %) in 2070 in UCT-INT compared to UCT-DIAG. As afforestation is a favored mitigation strategy under a UCT policy, we see a slight increase in afforestation and therefore albedo forcing under this more aggressive mitigation regime. However, the scale of changes in the fossil fuel sectors exceeds that in the land-use sectors.

Open image in new window

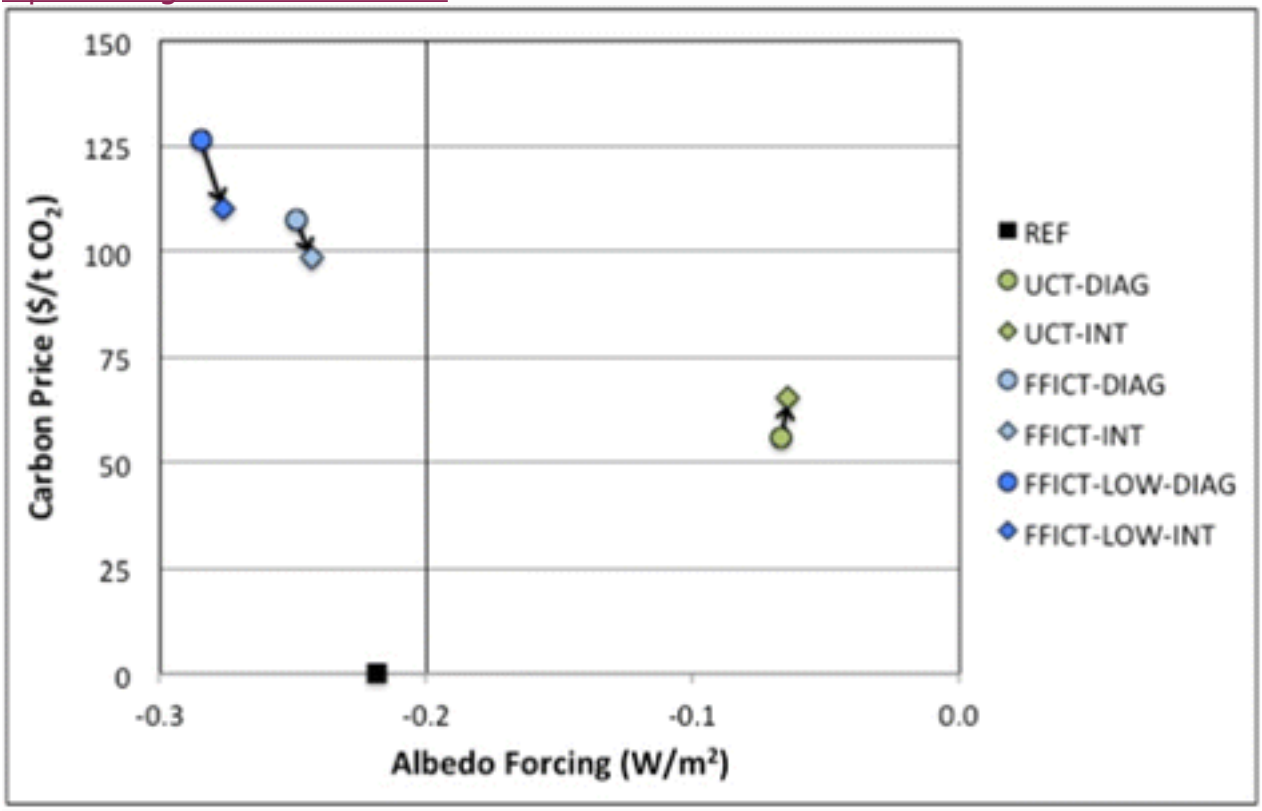

Fig. 4
Total global radiative forcing from albedo change in 2070 by scenario (x axis) versus the 2070 global carbon price required to meet scenario specific policy targets (y axis). Except for the reference scenario (REF), all scenarios reach a 4.5 W/m2 forcing target from all forcing agents considered. Diagnostic policy scenarios (-DIAG) do not include albedo forcing in the policy target, but interactive policy scenarios (-INT) do. The *vertical line* at −0.2 W/m^2 indicates the albedo forcing level in 2005 at the beginning of each simulation. *Black arrows* indicate the transition in this state space that occurs when albedo forcing is included in the target

Open image in new window

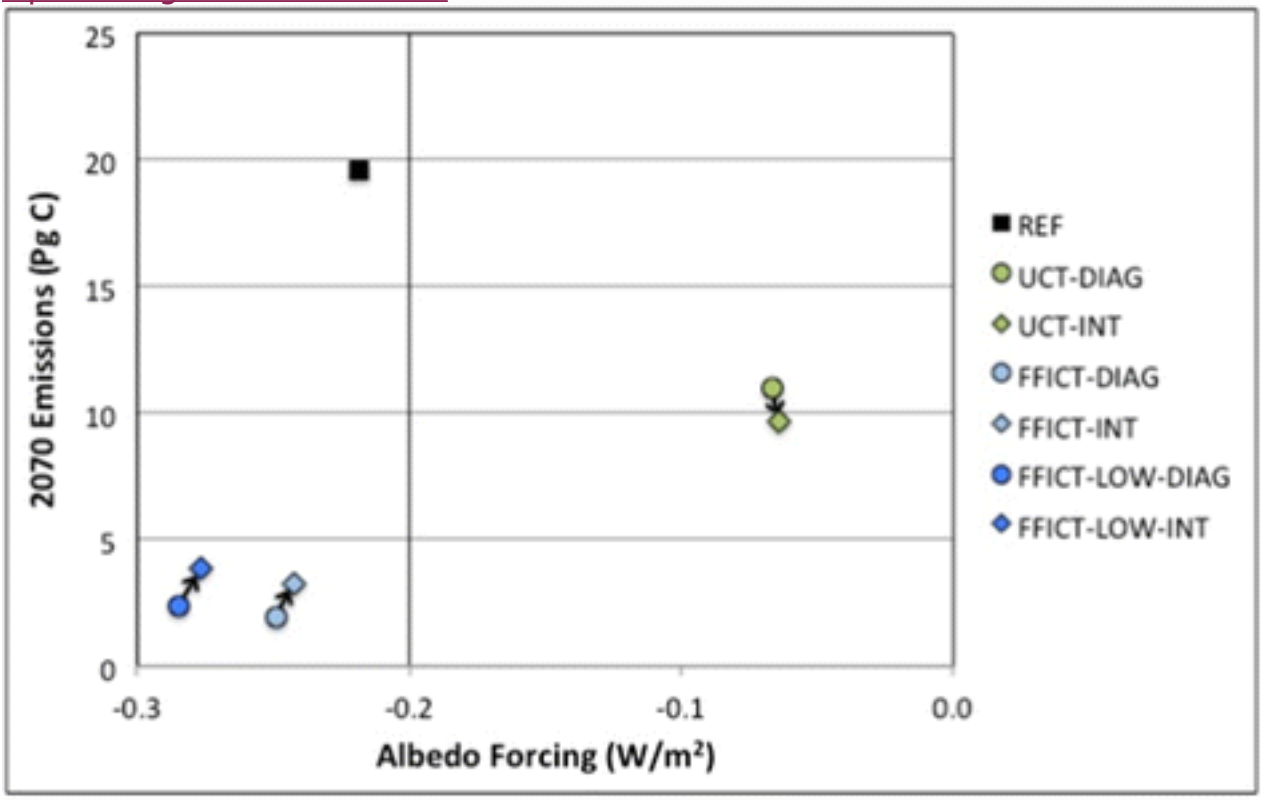

Fig. 5
Total global radiative forcing from albedo change in 2070 by scenario (x axis) versus 2070 global fossil fuel and industrial carbon emissions (y axis). Diagnostic policy scenarios (-DIAG) do not include albedo forcing in the policy target, but interactive policy scenarios (-INT) do. The *vertical line* at −0.2 W/m^2 indicates the albedo forcing level in 2005 at the beginning of each simulation. *Black arrows* indicate the transition in this state space that occurs when albedo forcing is included in the target

In the FFICT-INT and FFICT-LOW-INT scenarios, negative forcing due to deforestation makes the 4.5 W/m^2 target easier to meet. Thus, carbon prices decrease in these scenarios (Fig. 4), and fossil fuel emissions increase (Fig. 5). Fossil fuel emissions in 2070 are 1.3 PgC/yr (67 %) and 1.5 PgC/yr (62 %) higher in the FFICT-INT and FFICT-LOW-INT scenarios compared to the FFCIT-DIAG and FFICT-LOW-DIAG scenarios. As a percentage change, the fossil fuel emission changes in response to interactive albedo forcing are greater in the FFICT scenarios than the UCT scenarios due to the greater level of fossil fuel mitigation present in those scenarios. In the FFICT scenarios, bioenergy is a favored mitigation strategy and afforestation is not incentivized. Thus, with a reduced carbon price and correspondingly reduced pressure to mitigate, the need for bioenergy crops and land clearing decline in the FFICT-INT and FFICT-LOW-INT scenarios, yielding the observed increase in woody vegetation and albedo forcing.

Regional differences in LULCC and albedo forcing among the scenarios are apparent by examining Figs. 2 and 3. Most notably, a greater portion of the forest and shrubland cover change in the UCT scenarios comes from the Boreal AEZs (AEZ 13–18) compared to the FFICT scenarios. These Boreal AEZs are more strongly weighted in the albedo forcing calculation, whereas tropical AEZs are less strongly weighted. Despite the regional differences among scenarios, they are similar enough that cumulative land use change emissions is a good predictor of albedo forcing across all scenarios considered (Fig. 6).

Open image in new window

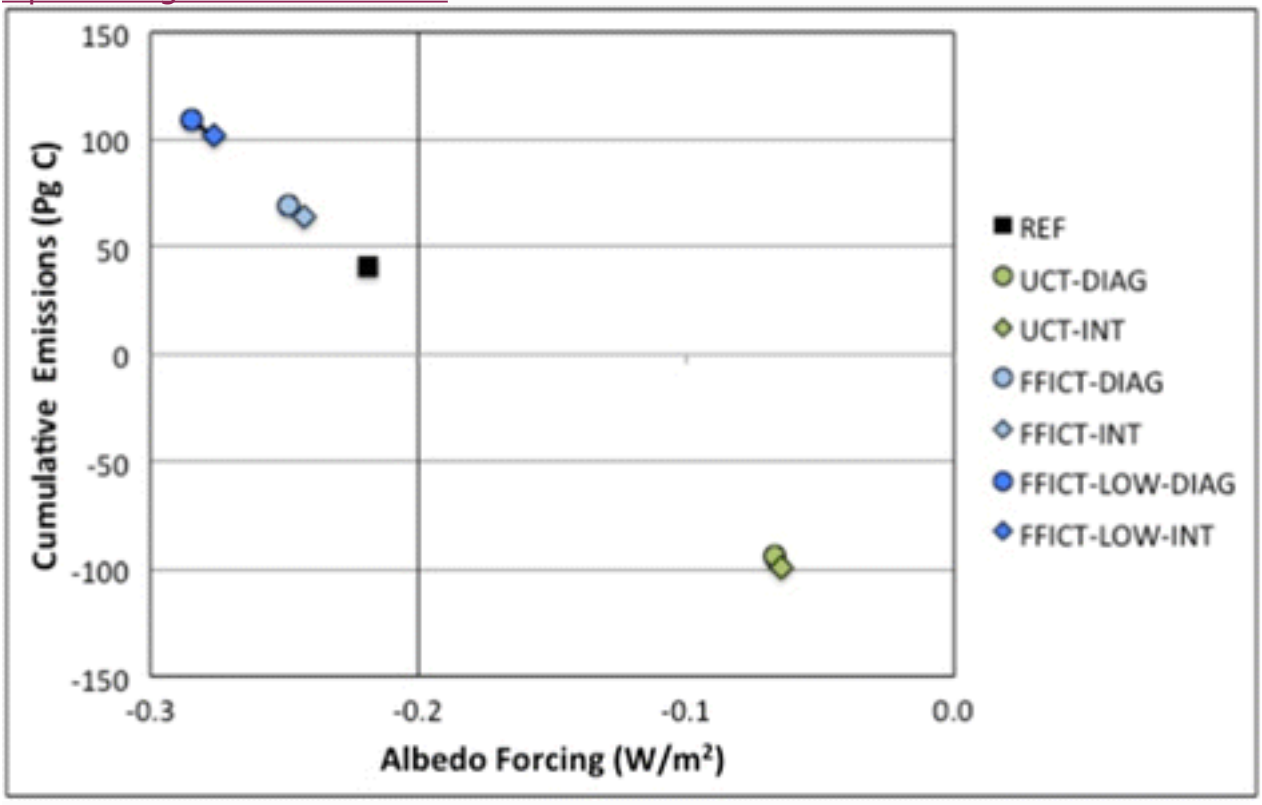

Fig. 6
Total global radiative forcing from albedo change in 2070 by scenario (x axis) versus cumulative (2005–2070) global emissions from land-use change (y axis). Diagnostic policy scenarios (-DIAG) do not include albedo forcing in the policy target, but interactive policy scenarios (-INT) do. The *vertical line* at −0.2 W/m^2 indicates the albedo forcing level in 2005 at the beginning of each simulation

4 Discussion

We demonstrate the viability of including spatially differentiated albedo forcing estimates within integrated assessment models, permitting us to diagnose the global scale of climate change resulting from this aspect of LULCC without the computationally expensive step of running climate and earth system models for each scenario of future human activity of interest.

This is a critical step toward producing more climatically consistent scenarios, as we can now distinguish scenarios with grossly different patterns of LULCC. In the scenarios that we consider, we find a range of future albedo forcing (~0 .25 W/m^2) that is similar in magnitude to central estimates for present-day forcing from halocarbons, nitrous oxide, carbon monoxide, and organic carbon aerosols (Stocker et al. 2013). .

Compared to previous work with the GCAM model (Wise et al. 2009; Calvin et al. 2014), we find a smaller range of future forest and shrub cover (and thus albedo forcing) across the UCT and FFICT scenarios. This is not entirely unexpected as we employ a newer version of GCAM featuring an AEZ-based approach to agriculture and land-use allocation. This newer version of GCAM uses more spatially explicit information and is less optimistic about the productivity of marginal lands overall and the willingness of landowners to cultivate those lands, than the previous version of GCAM.

Our method of accounting for albedo forcing also allows for the exploration of hypothetical policy scenarios in which non-greenhouse gas climate aspects of land-use change are valued. Including albedo forcing in the UCT and FFICT forcing targets affects mitigation dynamics, mostly through changes in fossil fuel emissions on the order of ~1.5 PgC/yr by 2070. Additional emissions cuts are needed in the UCT scenario to compensate for the warming effect of afforestation, whereas the opposite effect is found for the FFICT scenario.

We see only minor shifts in the overall magnitude or regional pattern of LULCC when including albedo forcing in the policy targets. To the extent that LULCC does change as a result of including albedo in the policy targets, forest and shrub cover is greater in all interactive scenarios compared to their diagnostic counterparts – a perhaps counterintuitive result given that removal of woody vegetation results in negative forcing and so would help to meet the targets. An explanation can be found by examining the dominant land-based mitigation strategy in the UCT and FFICT scenario families respectively. In the UCT scenarios, afforestation is a dominant strategy and additional forcing from this afforestation effectively tightens the target, requiring even more afforestation. In the FFICT scenarios, bioenergy is a dominant strategy and negative forcing from land clearing effectively loosens the policy target, requiring less bioenergy. We note, however, that we might find different results if we taxed albedo forcing directly rather than merely including it in the forcing targets, a next step that is certainly worth considering as this would be equivalent to valuing albedo forcing in terms of carbon dioxide equivalents, an approach that has been suggested in the literature on LULCC climate effects (Betts 2000; Caiazzo et al. 2014).

We emphasize, however, that global mean radiative forcing is not a perfect metric for characterizing the full spatially differentiated climate effects of LULCC. Some studies imply a modest local warming effect of tropical deforestation (e.g., (Arora and Montenegro 2011)), yet our radiative forcing factors for clearing woody vegetation are less than zero in all regions. This is because some climate effects of LULCC cannot be quantified in terms of radiative forcing (e.g., hydrological effects) (Pielke et al. 2002), and these effects tend to dominate over albedo effects in the tropics (Bonan 2008). Another challenge follows from the regional scope of LULCC climate effects compared to well-mixed greenhouse gases. Modeling studies have shown that adding radiative forcing from LULCC and greenhouse gases can lead to counter-intuitive climate outcomes, especially in terms of regional patterns of change (Jones et al. 2013b). Similar shortcomings have been noted for radiative forcing from aerosols as well (Edmonds and Wise 1999; Anon 2005).

A move away from global forcing metrics toward producing spatially and temporally resolved climate change signals using pattern scaling (Mitchell 2003; Tebaldi and Arblaster 2014) or some other form of reduced-form climate modeling would provide a means to better understand the climate implications of different scenarios of future human activity. However, as long as global mean radiative forcing remains the dominant paradigm for characterizing the strengths of climate perturbations, the method we present here provides a mechanism to treat LULCC in a consistent manner as other forcing agents while indicating the overall scale of LULCC climate effects – a major advance over previous methods that essentially ignored the non-CO_2 effects of LULCC on climate.

As a next step, our method could be improved by considering more land cover classes, by considering forcing estimates based on a wider variety of earth system models, or by including direct satellite observations of surface albedo in the forcing calculation. Finally, we note that future changes in snow cover as a result of global climate change will alter the radiative effect of landcover change, particularly at high latitudes. Since this approach is based on static forcing factors, the effect of changing snow climatologies is not captured. One approach to addressing this would be to derive separate factors that correspond to different levels of global mean temperature change, a quantity that is typically estimated within integrated assessment models based on global forcing and an assumed climate sensitivity.

Footnotes

1. 1.

The IAMs used to generate the RCPs do include radiative forcing from historic albedo change. However, this forcing is held constant at −0.2 W/m2

throughout the 21st century, regardless of future LULCC. For the RCPs, this historic albedo forcing was not included in the totals reported or used to drive the internal climate policies.

2. 2.

We focus our analysis on the year 2070 in part because the GCAM model exhibits non-convergent behavior beyond this point for the FFICT scenarios See Calvin et al. (2014) for a description of this phenomenon.

Notes

Acknowledgments

This research was supported by the Office of Science of the U.S. Department of Energy as part of the Improving the Representations of Human-Earth System Interactions Project. This work used the Community Earth System Model, CESM and the Global Change Assessment Model, GCAM. The National Science Foundation and the Office of Science of the U.S. Department of Energy support the CESM project. The authors acknowledge long-term support for GCAM development from the Integrated Assessment Research Program in the Office of Science of the U.S. Department of Energy. This research used resources of the National Energy Research Scientific Computing Center, which is supported by the Office of Science of the U.S. Department of Energy under Contract No. DE-AC02-0 5CH11231. Battelle Memorial Institute operates the Pacific Northwest National Laboratory for DOE under contract DE-AC06-76RLO 1830. Lawrence Berkeley National Laboratory is supported by the U.S. Department of Energy under Contract No. DE-AC02-0 5CH11231.

References

1. Anon (2005) Radiative forcing of climate change: expanding the concept and addressing uncertainties. National Acad Sciences. [online] Available from: http://www.nap.edu/openbook.php?record_id=11175

2. Arora VK, Montenegro A (2011) Small temperature benefits provided by realistic afforestation efforts. Nat Geosci 4:514–518CrossRefGoogle Scholar

3. Bala G, Caldeira K, Wickett M et al (2007) Combined climate and carbon-cycle effects of large-scale deforestation. Proc Natl Acad Sci 104:6550CrossRefGoogle Scholar

4. Ban-Weiss GA, Cao L, Bala G, Caldeira K (2011) Dependence of climate forcing and response on the altitude of black carbon aerosols. Climate Dynam 38:897–911. doi: 10.1007/s00382-011-1052-yCrossRefGoogle Scholar

5. Betts R (2000) Offset of the potential carbon sink from boreal forestation by decreases in surface albedo. Nature 408:187–190CrossRefGoogle Scholar

6. Bonan G (2008) Forests and climate change: forcings, feedbacks, and the climate benefits of forests. Science 320:1444–1449. doi: 10.1126/science.1155121CrossRefGoogle Scholar

7. Brovkin V, Boysen L, Arora VK et al (2013) Effect of anthropogenic land-use and land-cover changes on climate and land carbon storage in CMIP5 projections for the twenty-first century. J Climate 26:6859–6881. doi: 10.1175/JCLI-D-12-00623.1CrossRefGoogle Scholar

8. Caiazzo F, Malina R, Staples MD et al (2014) Quantifying the climate impacts of albedo changes due to biofuel production: a comparison with biogeochemical effects. Environ Res Lett 9:024015. doi: 10.1088/1748-9326/9/2/024015CrossRefGoogle Scholar

9. Calvin K, Clarke L, Edmonds J, Eom J, Hejazi M, Kim S, Kyle P, Link R, Luckow P and Patel P (2011) “GCAM Wiki Documentation.” from https://wiki.umd.edu/gcam/

10. Calvin K, Wise M, Clarke L et al (2014) Near-term limits to mitigation: challenges arising from contrary mitigation effects from indirect land-use change and sulfur emissions. Energy Econ 42:233–239. doi: 10.1016/j.eneco.2013.09.026CrossRefGoogle Scholar

11. Conley AJ, Lamarque JF, Vitt F et al (2013) PORT, a CESM tool for the diagnosis of radiative forcing. Geosci Model Dev 6:469–476CrossRefGoogle Scholar

12. Davies-Barnard T, Valdes PJ, Singarayer JS, Jones CD (2014) Climatic impacts of land-use change due to crop yield increases and a universal carbon Tax from a scenario model. J Climate 27:1413–1424CrossRefGoogle Scholar

13. Edmonds J, Wise M (1999) Exploring A Technology Strategy for Stabilizing Atmospheric CO2. International Environmental Agreements on Climate Change, Kluwer Academic Publishers 131–154Google Scholar

14. Feddema JJ, Oleson KW, Bonan GB et al (2005) The importance of land-cover change in simulating future climates. Science 310:1674–1678. doi: 10.1126/science.1118160CrossRefGoogle Scholar

15. Foley J, DeFries R, Asner G, Barford C (2005) Global consequences of land use. Science 309:570–574CrossRefGoogle Scholar

16. Hallgren W, Schlosser CA, Monier E et al (2013) Climate impacts of a large-scale biofuels expansion. Geophys Res Lett 40:1624–1630. doi: 10.1002/grl.50352CrossRefGoogle Scholar

17. Hurrell JW, Hack JJ, Shea D et al (2008) A new sea surface temperature and sea ice boundary dataset for the community atmosphere model. J Climate 21:5145–5153CrossRefGoogle Scholar

18. Hurrell JW, Holland MM, Gent PR et al (2013) The community earth system model: a framework for collaborative research. Bull Am Meteorol Soc 94:1339–1360CrossRefGoogle Scholar

19. Iacono MJ, Delamere JS, Mlawer EJ et al (2008) Radiative forcing by long-lived greenhouse gases: calculations with the AER radiative transfer models. J Geophys Res 113:D13103CrossRefGoogle Scholar

20. Jones AD, Collins W, Edmonds J et al (2013a) Greenhouse gas policies influence climate via direct effects of land use change. J Climate 26:3657–3670. doi: 10.1175/JCLI-D-12-00377.1CrossRefGoogle Scholar

21. Jones AD, Collins WD, Torn MS (2013b) On the additivity of radiative forcing between land use change and greenhouse gases. Geophys Res Lett 40:4036–4041. doi: 10.1002/grl.50754CrossRefGoogle Scholar

22. PJ, Chase TN (2007) Representing a new MODIS consistent land surface in the Community Land Model (CLM 3.0). J Geophys Res 112:G01023. doi: 10.1029/2006JG000168

23. Lawrence DM, Oleson KW, Flanner MG et al. (2011) Parameterization improvements and functional and structural advances in Version 4 of the Community Land Model. J Adv Model Earth Syst. 3:1–27. doi: 10.1029/2011MS000045

24. Lee H-L, Hertel T, Sohngen B, Ramankutty N (2005) Towards an integrated land use data base for assessing the potential for greenhouse gas mitigation. GTAP Technical Papers 25. 1–83. https://www.gtap.agecon.purdue.edu/resources/res_display.asp?RecordID=1900

25. Meinshausen M, Raper S, Wigley T (2011) Emulating coupled atmosphere–ocean and carbon cycle models with a simpler model, MAGICC6–Part 1: Model description and calibration. Atmos Chem Phys 11:1417–1456CrossRefGoogle Scholar

26. Mitchell TD (2003) Pattern scaling: an examination of the accuracy of the technique for describing future climates. Clim Change 60:217–242. doi: 10.1023/A:1026035305597CrossRefGoogle Scholar

27. Monfreda C, Ramankutty N, Hertel TW (2009) Global agricultural land use data for climate change analysis. In: Hertel T, Rose S, Tol R (eds) Economic analysis of land use in global climate change policy. Routledge, UKGoogle Scholar

28. Park S, Bretherton CS, Rasch PJ (2014) Integrating cloud processes in the community atmosphere model, version 5. J Climate 27:6821–6856. doi: 10.1175/JCLI-D-14-00087.1CrossRefGoogle Scholar

29. Pielke R Sr, Marland G, Betts R et al (2002) The influence of land-use change and landscape dynamics on the climate system: relevance to climate-change policy beyond the radiative effect of greenhouse gases. Philos Trans R Soc 360:1705–1719CrossRefGoogle Scholar

30. Pongratz J, Reick CH, Raddatz T, Claussen M (2010) Biogeophysical versus biogeochemical climate response to historical anthropogenic land cover change. Geophys Res Lett. doi: 10.1029/2010GL043010Google Scholar

31. Pongratz J, Reick CH, Raddatz T et al (2011) Past land use decisions have increased mitigation potential of reforestation. Geophys Res Lett 38:L15701Google Scholar

32. Stocker TF, Qin D, Plattner GK et al (2013) IPCC, 2013: Climate Change 2013: the physical science basis. Contribution of working group I to the fifth assessment report of the intergovernmental panel on climate. Cambridge University Press, ChangeGoogle Scholar

33. Taylor KE, Stouffer RJ, Meehl GA (2012) An overview of CMIP5 and the experiment design. Bull Am Meteorol Soc 93:485–498CrossRefGoogle Scholar

34. Tebaldi C, Arblaster JM (2014) Pattern scaling: its strengths and limitations, and an update on the latest model simulations. Clim Change 122:459–471. doi: 10.1007/s10584-013-1032-9CrossRefGoogle Scholar

35. Thomson AM, Calvin KV, Smith SJ et al (2011) RCP4. 5: a pathway for stabilization of radiative forcing by 2100. Clim Change 109:77–94CrossRefGoogle Scholar

36. van Vuuren DP, Edmonds J, Kainuma M et al (2011) The representative concentration pathways: an overview. Clim Change 109:5–31. doi: 10.1007/s10584-011-0148-zCrossRefGoogle Scholar

37. Wise M, Calvin K, Thomson A et al (2009) Implications of Limiting CO2 Concentrations for Land Use and Energy. Science 324:1183–1186. doi: 10.1126/science.1168475CrossRefGoogle Scholar

38. Wise M, Calvin KV, Kyle P et al (2014) Economic and physical modeling of land Use in GCAM 3.0 and an application to agricultural productivity, land, and terrestrial carbon. Clim Change Econ 05:1450003. doi: 10.1142/S2010007814500031CrossRefGoogle Scholar